State diagrams of arabinoxylan-water binaries

Dimitrios Fessas[*], Alberto Schiraldi

DISTAM, University of Milan, Via Celoria 2, 20133 Milano, Italy

Abstract

Since Arabinoxylans are natural polysaccharides that seem promising candidates as cryostabilizers, the state diagram (i.e. the representation in the temperature-composition plan of the macroscopic phases) of their aqueous solutions seemed worth determining.

Two lots of purified water extractable arabinoxylans (WEA) of different molecular mass (56 and 410 kDa labeled as LMW-AX and HMW-AX, respectively) were used to prepare aqueous solutions of various composition. These were cooled below their freezing point and annealed for 2 h at a suitable temperature before a DSC 5°C min^{-1} heating run aimed at determining their primary glass transition temperature, T'_g, and the onset of ice fusion. Once the corresponding composition, C'_g, was assessed, the main curves of the corresponding state diagram were drawn.

As expected, the T'_g value drawn for HMW-AX was higher (-17°C) than for LMW-AX (-35°C). The C'_g was instead found close to 75% w/w for both HMW-AX and LMW-AX. The fictitiousness of this coincidence could be easily recognized by expressing the solute concentration in molar fraction, X: it was then possible to verify that, as expected, X'_g for LMW-AX was one order of magnitude larger than for HLW-AX. © 2001 Elsevier Science B.V. All rights reserved.

Keywords: Cryostability; Arabinoxylans; Pentosans; State diagrams; DSC

1. Introduction

Pentosans are non-starch polysaccharides found in the starchy endosperm and aleurone cell walls of many cereals [1–3]: more precisely, they are Arabinoxylans (AX) and Arabinogalactans (AG) [4–9]. Pentosans are supposed to play some role in bread making, since their addition to standard dough recipes can affect the sensorial quality and the shelf life of the baked product. Literature on pentosans is, therefore, abundant although rather confuse about the specific role of these polymers, because of the large discrepancies between the opinions of different authors. Most of them concur in concluding that water insoluble pentosans are detrimental for the bread quality, while no unambiguous conclusion can be drawn from the reports about water soluble pentosans [10–20]. A main issue of debate concerned the interactions between pentosans and other dough components, namely starch and gluten, whereas a general consensus received the statement that these polymers can trap large amounts of water, although literature does not report any specific investigation about this important property [21–27].

Such contradictions can be nowadays explained with a number of arguments, like, for example, the superposition of the effects produced by AG to those due to AX, the molecular mass distribution (possibly due to different enzymatic activity of endogenous

---

[*] Corresponding author. Tel.: +390-2-70-60-2063;
fax: +390-2-70-63-8625.
E-mail address: dimitrios.fessas@unimi.it (D. Fessas).

hemicellulases), and the very important acknowledgement that pentosans are thermodynamically uncompatible versus proteins and starch polysaccharides, which means that they tend to form a separate aqueous phase interdispersed with those hosting the other dough polymers [28–31].

These findings underlie a new deal of investigations which nowadays tend to split the role of AG from that of AX and are based on the principles of polymer and colloidal sciences, which include the glass transition temperature, T_g, as an index of molecular mobility, and water exchanges between dispersed phases hosting different hydrophilic polymers [32–34]. A further issue to be considered is the balance between the opposite effects related to the molecular mass and the branching degree on the solubility and the viscosity of the hosting system.

With the aim at defining a more comprehensive picture of AX properties, a number of investigations were undertaken in our laboratory [35]. The AX primary molecular structure can be described as a long chain of xylose moieties (1-2 β glycosidic bonds) with some side branches formed by single arabinose units (1-2 and/or 1-3 α glycosidic bonds). Chain length and branching degree affect their solubility in water, and therefore, the possibility to extract them from the original flour. Accordingly, they have been naively referred as to water-extractable and water-unextractable AX (WEA and WUA, respectively). The WUA have molecular mass exceeding 10^6 Da, while WEA are spread over a wide molecular mass range spanning from 10^3 to 10^6 Da. This dispersion is a result of the activity of endogenous xylanases and xylanase inhibitors present in the original cereals [36–39].

The WEA seem promising candidates as cryostabilizing agents in food and drug preparations, since their aqueous solutions, even at a concentration of 0.5% (w/w), have a viscosity which hinders the growth of ice crystals on cooling [40–42]. This property, however, depends on the average molecular mass of the polymers and their hydrophilic character, as well as on temperature. The actual cryostabilization potential of WEA has, therefore, to be checked at temperatures below the freezing point of the system to stabilize. Neither detailed investigations about these polymers at sub-ambient temperature, nor any specific study about their hydrophilic behavior are reported in the literature.

The present work deals with the determination of the state diagrams of the AX-H_2O binaries and aims at defining the freezing behavior of WEA, their glass transition temperature, and the effect of the molecular mass on these properties, using polymers of similar brancing degree.

2. Materials and methods

The AX considered are purified WEA of different molecular mass [43], which were supplied by the laboratory of Food Chemistry of the Catholic University of Leuven (Belgium) together with the relevant composition (see Table 1).

Based on the GLPC records, also received from Leuven, the molecular mass dispersion of the two WEA lots were drawn for the present work (see Fig. 1).

The weight and the number average molecular masses, and the dispersion degree

$$M_w = \frac{\sum n_i M_i^2}{\sum n_i M_i}, \qquad M_n = \frac{\sum n_i M_i}{\sum n_i},$$
$$\text{and} \qquad d = \frac{M_w}{M_n}$$

were accordingly evaluated for either WEA lot (see Table 2), n_i being the number fraction observed for each molecular mass M_i in the dispersion reported in Fig. 1.

The lower molecular mass WEA showed a rather spread distribution, while a much narrower dispersion was found for the other WEA lot. In spite of these differences, the two WEA lots might be referred to as belonging to significantly distinct ranks of molecular masses, which were named low and high molecular mass WEA (LMW and HMW) for the present work. Any further separation into more homogeneous

Table 1
Composition of WEA[a]

	LMW-AX	HMW-AX
AX (%) (w/w dry matter)	86.0	94.7
AG (%) (w/w dry matter)	6.1	3.8
Arabinose/xylose	0.66	0.51

[a] The rest of dry matter is mainly formed by glucose and proteins. Moisture content was about 3% (w/w of the lyophilized powder) for both WEA.
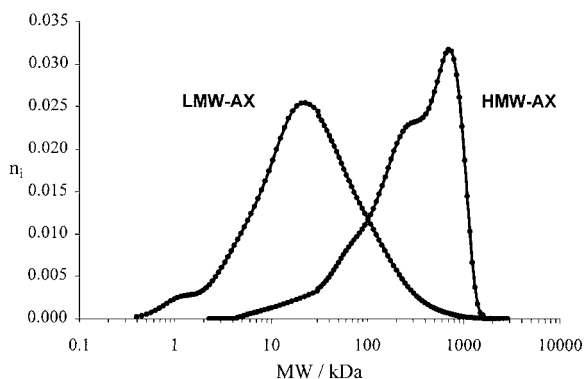
Fig. 1. Molecular mass dispersion of the two arabinixylan lots (LMW-AX and HMW-AX), with $\sum n_i = 1$.

classes was not considered, in as much as the technical interest for pentosans concern samples with this kind of dispersion and their effects on the cryostability of systems.

The two lots were used to prepare aqueous solutions at various compositions (1–85% w/w).

The DSC measurements were performed by a Pyris 1 DSC (Perkin-Elmer) with automatic liquid N_2 (CryoFill) coolling mode operating across the -150, $100°C$ range. About 30 mg samples in sealed (maximum pressure 24 atm) stainless steel pans (maximum volume 60 µl) were used. Indium was used for calibration. Before every DSC heating run (-80, $20°C$ at $5°C \, min^{-1}$), the sample has undergone 2 h annealing at a temperature, tentatively assumed just above the T'_g (see bellow) to allow ice crystallization to take place and after was been cooled to $-80°C$ at $10°C$ cooling rate and stay for 15 min. The raw data were treated by means of the Pyris Software for Windows version 3.71, (Perkin-Elmer LLC) and by the dedicated software IFESTOS [44] which was assembled by the authors for handling raw calorimetric data according to the suggestions by Barone et al. [45]

Table 2
Number, weight average molecular masses and dispersion degree of WEA

	LMW-AX (kDa)	HMW-AX (kDa)
M_n	56	410
M_w	235	650
d	4.2	1.6

to obtain the apparent heat capacity of the sample, $C_p^{app}(T)$/J K^{-1} g^{-1} (per gram of solution).

3. General considerations

Most water soluble food ingredients produce a cryoscopic effect and may be, therefore, expected to form simple eutectic binary systems when mixed with water [46]. This is not the case when the solute is a polymer, since the increased concentration of the liquid phase, due to the primary ice separation, is accompanied by an increase of viscosity, which reduces and eventually inhibits the formation of ice crystals. Any further cooling produces a glassy state where the molecular mobility of either component of the binary is severely limited [47–49]. The lowest temperature at which a liquid is still present is commonly indicated as T'_g and the corresponding solute concentration as C'_g. The point (T'_g, C'_g) can be far away from the eutectic point predicted by equilibrium thermodynamics, but it practically mimics a true invariant point as long as, if the cooling rate is sufficiently low, for any solute concentration C in the range $0 < C < C'_g$, ice crystals are formed on cooling across the relevant freezing point, and the solute concentration of the residual liquid phase eventually attains the value C'_g at $T = T'_g$. Below this temperature the system is a mechanical mixture of ice crystals dispersed within a glass matrix of C'_g composition. When these frozen systems are thawed, a C'_g liquid phase appears at $T = T'_g$, which is also the onset temperature of the ice fusion [50].

For very high cooling rates no ice is separated and, at a temperature $T_g < T'_g$, the system turns into a homogeneous glass phase with the same composition as the starting liquid solution. This direct transition from liquid to glass state occurs at any cooling rate when the starting solution has a concentration $C = C'_g$. This means that the point (C'_g, T'_g) belongs to the curve $T_g = T_g(C)$ which describes the trend of the glass transition temperature, T_g, versus C. The $T_g(C)$ trend can be reported in the so called *state diagram* of the binary together with the curves relevant to primary ice separation and polymer solubilization [50].

The state diagram (see Fig. 2) of a polymer-water binary is the representation of the macroscopic phases, including the glassy ones, formed as a consequence of
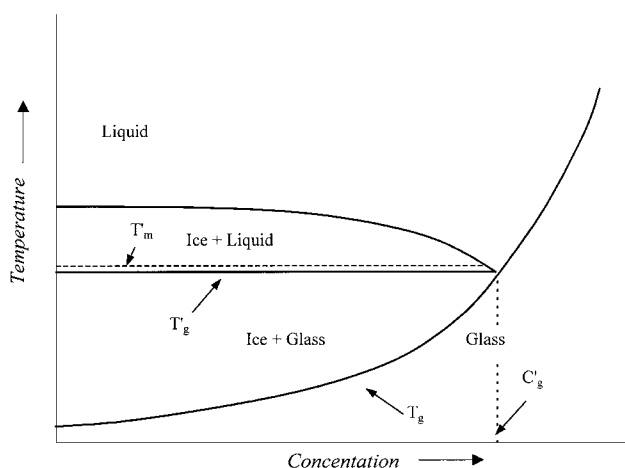
Fig. 2. State diagram of a polymer-water binary.

heating/cooling and/or dehydration treatments, which can have very long relaxation times (months, years or centuries). The T_g relevant to a given composition represents the threshold above which molecular displacements, which are "frozen" below T_g, can take place (with increase of the system heat capacity) and sustain the progress of chemical and/or physical transformations, like nucleation and growth of thermodynamically stable phases.

Standard DSC investigations allow determination of the $T_g = T_g(C)$ trend when $C > C_g'$, since the relevant traces are not affected by ice fusion [51].

Specially equipped instruments and a mathematical treatment of the trace are instead necessary to investigate the $C < C_g'$ range. In this case, (if the samples were annealed before the DSC run just above a tentatively estimated T_g' so as to allow the maximum ice formation and avoid exothermic peaks related to ice crystallization of super-cooled water above the T_g'), the DSC trace shows an endothermic base line shift whose middle point temperature is a reasonable estimation of T_g'.

Even more difficult is the determination of T_g for any $C < C_g'$, since it requires a very fast quenching ($>10^8\ \mathrm{K\ min^{-1}}$) of the sample down to very low temperatures (e.g. -100°C) so as to avoid ice crystallization on cooling. It is, therefore, a common practice to experimentally determine the $T_g(C)$ trend for $C \geq C_g'$ and extrapolate the fit down to the glass transition of pure water, $T_g(H_2O) = -140^\circ$C, with use of some empirical equation.

4. Results and discussion

For both LMW-AX and HMW-AX solutions T_g' and C_g' were determined with DSC investigations performed on 2 h annealed samples (see above). Fig. 3 shows typical DSC records obtained in this work. The endothermic base line shift (see insert in the figure) preceding the endothermic peak of ice fusion was attributed to the prime glass transition and the temperature at its middle point was considered a reasonable estimation of T_g'. As expected this value remained constant (within a $\pm 2^\circ$C error) throughout a wide composition range. The relatively large temperature range encompassed by this base line shift is a consequence of the actual dispersion of the molecular mass (see Fig. 1): it was indeed found that this temperature range was wider for LMW-AX than for HMW-AX.

Ice melting started after the T_g' drift and produced a shouldered peak. Samples with a large C gave DSC traces where the base line shift at T_g' was followed by an exothermic poach, related to the formation of ice crystals (namely, a fraction of those not formed during the annealing, probably because of the large viscosity of these systems), which was partially overlapped to the endothermic peak of ice melting. The overall signal across T_g' was, therefore, not suitable to quantitatively evaluate the amount of "freezable" water and, as a consequence, to determine C_g' with few experiments. As a reasonable experimental compromise, a large number of partially (2 h were evidently
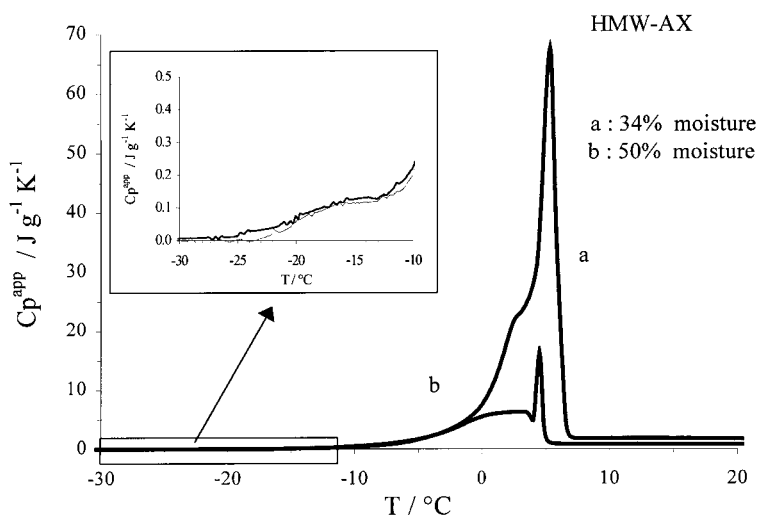
Fig. 3. The DSC records from aqueuss solutions of high molecular weight arabinoxylans (HMW-AX) at two different water contents.

not sufficient) annealed samples with different solute concentration were examined, so as to determine the T'_g value, which was expected not to change with the composition. The value of C'_g was singled out from the data relevant to 10 different compositions (data in Figs. 4 and 5), for either WEA lot, as the largest solute concentration at which the shift of the base line of the DSC trace at T'_g was not accompanied by any endothermic signal related to ice fusion.

The enthalpy of ice fusion was not evaluated, since the samples were not annealed as long as to guarantee the maximum formation of ice crystals prior to the

DSC heating run (see above). The shape of the corresponding peak was indeed complex, suggesting either the presence of ice crystals of different size, or a partially overlapped exothermic effect due to the formation of new ice crystals (see above). Nevertheless the onset point of this signal did not depend on the AX concentration, C, but, as expected, its intensity and end temperature decreased on increasing C.

It was noticed that the onset of ice fusion appeared just after T'_g for HMW-AX, whereas it was delayed in the case of LMW-AX and could be given a clearly separated temperature, which, for the sake
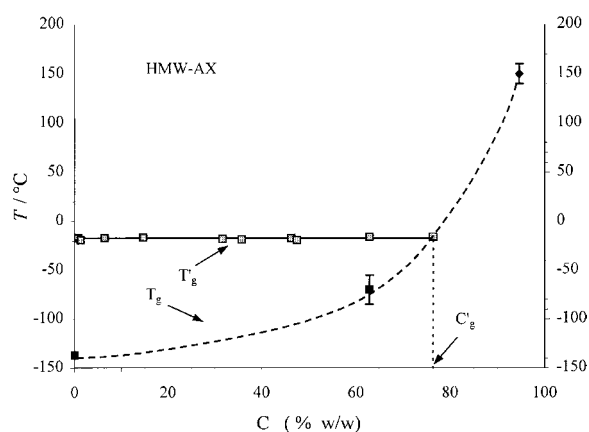

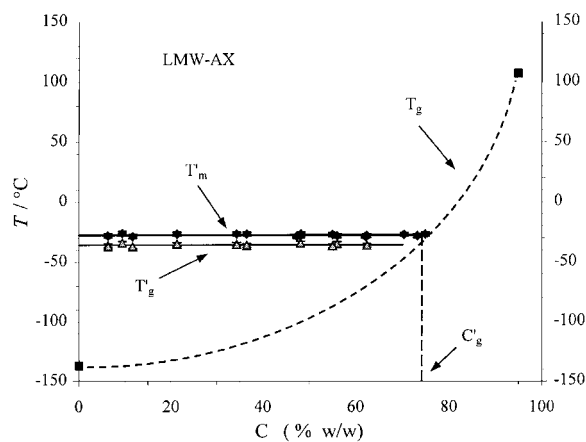Fig. 4. State diagram of HMW-AX water solutions.
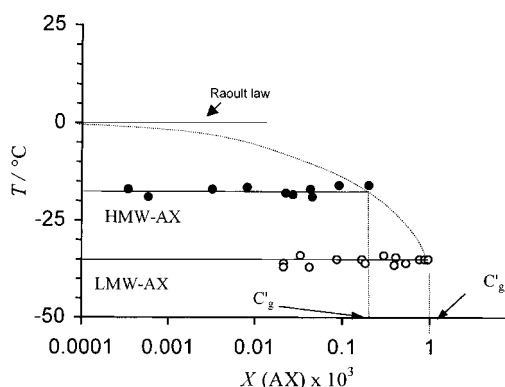

Fig. 5. State diagram of LMW-AX water solutions.

Fig. 6. State diagrams for HMW-AX end LMW-AX water solutions where concentration is given as molar fraction (assuming the number average molecular weight M_n).

of comparison with similar findings reported in the literature, was labeled as T'_m [50]. Such a delay was probably related to a mismatch between the heating rate used in DSC runs and the rate of fusion of ice crystals and might be considered partially fictitious because of the wide temperature range of the LMW-AX glass transition (and therefore, the broad molecular mass distribution of this lot).

As expected, the T'_g value drawn for HMW-AX was higher ($-17°C$) than for LMW ($-35°C$), while C'_g was found close to 75% w/w for both HMW-AX and LMW-AX. All these experimental data where reported in the relevant state diagrams (Figs. 4 and 5). The T_g curve across the whole diagram was tentatively drawn as a SP line passing through three points, namely $T_g(H_2O)$, (T'_g, C'_g) and another point obtained either from a rapidly quenched solution with $C > C'_g$ (for HMW-AX), or from a partially dehydrated sample (LMW-AX).

The coincidence of the C'_g for either system was easily recognized as a fictitious finding as long as the expected split appeared when the solute concentration was replaced with the corresponding molar fraction, X, evaluated according to the relevant M_n (Fig. 6). The X'_g (replacing C'_g) for LMW-AX was almost one order of magnitude larger than for HLW-AX.

This seemed reasonable since the maximal freeze concentration of the liquid phase is directly related to its viscosity at T'_g. At a given temperature, the viscosity of a polymer solution depends on the molecular mass of the polymer and, for a given series

of homologous polymers, like LMW-AX and HMW-AX, the viscosity at a given solute mass % content should follow the empirical law, $\eta \propto \log M_w$ [51]. Since the event that takes place at T'_g is the inhibition of ice segregation in either system, a reliable expectation was that such a condition would be met at a lower X for HLM-AX than for LMW-AX. This consideration was largely qualitative, since it did not account for the effect of the temperature; nevertheless, in the present case, this effect could be comparable in either system, so as to enhance the role of the molecular mass of the solute.

5. Conclusions

The present study was performed on water soluble arabinoxylans which have different molecular mass, but similar branching degree (about 0.5 (private communication)); other soluble arabinoxylans can, however, be obtained by chemical and/or enzymatic cleavage of the insoluble fraction of wheat fibers: these should have larger molecular mass but also different branching degree. With respect to the viscosity and T'_g of the hosting system, differences related to the molecular mass, such as those observed in the present work (better cryostabilizing potential coupled with a larger molecular mass), could follow a different trend, since the effects of the molecular mass could be counterbalanced by those related to the branching degree. Further work is, therefore, necessary to split the two effects and obtain a more complete characterization of these polymers.

References

[1] R. Amado, H. Neukom, in: R.D. Hill, L. Menck (Eds.), New Approaches to Research on Cereal Carbohydrates, Elsevier, Amsterdam, 1985, p. 241.

[2] F. Meuser, P. Suckow, in: J.M.V. Blanshard, P.J. Frazier, T. Galliard (Eds.), Chemistry and Physics of Baking, The Royal Society of Science, London, 1986, p. 42.

[3] K. Autio, in: A.C. Eliasson (Ed.), Carbohdyrates in Food, Marcel Dekker, New York, 1996, p. 227.

[4] M. Izydorczyk, C.G. Biliaderis, W. Bushuk, Cereal Chem. 68 (1991) 139.

[5] M.S. Izydorczyk, C.G. Biliaderis, W. Bushuk, Cereal Chem. 68 (1991) 145.

[6] M.S. Izydorczyk, C.G. Biliaderis, J. Agric. Food Chem. 40 (1992) 561.

[7] M.S. Izydorczyk, C.G. Biliaderis, Carbohydr. Polym. 17 (1992) 237.

[8] M.S. Izydorczyk, C.G. Biliaderis, Cereal Chem. 70 (1993) 641.

[9] M.S. Izydorczyk, C.G. Biliaderis, Carbohydr. polym. 28 (1995) 33.

[10] R.W. Cawley, J. Food Agric. 15 (1964) 834.

[11] S.L. Jelaca, I. Hlynka, Cereal Chem. 49 (1972) 489.

[12] S.K. Kim, B.L. D'Appolonia, Cereal Chem. 40 (1977) 823.

[13] S.K. Patil, K.F. Finney, M.D. Shogren, C.C. Tsen, Cereal Chem. 53 (1976) 347.

[14] R.C. Hoseney, Food Technol. 38 (1984) 114.

[15] M. Jankiewicz, J. Michniewicz, Food Chem. 25 (1987) 241.

[16] J. Michniewics, C.G. Biliaderis, W. Bushuk, Cereal Chem. 68 (1991) 252.

[17] J. Michniewics, C.G. Biliaderis, W. Bushuk, Food Chem. 43 (1992) 251.

[18] S. Vanhamel, G. Cleemput, J.A. Delcour, M. Nys, P.L. Darius, Cereal Chem. 70 (1993) 306.

[19] C.G. Biliaderis, M.S. Izydorczyk, O. Rattan, Food Chem. 53 (1995) 165.

[20] S.K. Kim, B.L. D'Apolonia, Cereal Chem. 54 (1977) 225.

[21] B.L. D'Appolonia, K.A. Gilles, D.G. Medcalf, Cereal Chem. 47 (1970) 194.

[22] M. Gudmundsson, A.C. Eliasson, S. Bengtsson, P. Aman, Starch 43 (1991) 5.

[23] M. Gudmundsson, A.C. Eliasson, S. Bengtsson, P. Åman, Starch/Stärke 43 (1991) 5.

[24] J.A. Delcour, S. Vanhamel, R.C. Hoseney, Cereal Chem. 68 (1991) 72.

[25] J.A. Delcour, S. Vanhamel, R.C. Hoseney, Cereal Chem. 68 (1991) 72.

[26] L. Saulnier, N. Peneau, J.F. Thibault, J. Cereal Sci. 22 (1995) 259.

[27] G. Cleemput, C. Booij, M. Hessing, H. Gruppen, J.A. Delcour, J. Cereal Sci. 26 (1997) 55.

[28] V. Tolstoguzov, Food Hydrocolloids 4 (1991) 429.

[29] H. Larson, A.C. Eliasson, Cereal Chem. 73 (1996) 18.

[30] G.V. Ya, V.B. Tolstoguzov, Food Hydrocolloids 11 (1997) 145.

[31] C.B. Closs, B. Conde-Petit, I.D. Roberts, V.B. Tolstoguzov, F. Escher, Carbohydrate Polym. 39 (1999) 67.

[32] J.W. Donovan, Biopolymers 18 (1979) 263.

[33] K.J. Zeleznak, R.C. Hoseney, Cereal Chem. 64 (1987) 121.

[34] Y. Roos, M. Karel, J. Food Sci. 56 (1991) 38.

[35] D. Fessas, A. Schiraldi, Thermochim. Acta 323 (1998) 17–26.

[36] G. Cleemput, C. Booij, M. Hessing, H. Gruppen, J.A. Delcour, J. Cereal Sci. 26 (1997) 55.

[37] A.S. Perlin, Cereal Chem. 28 (1951) 382.

[38] X. Rouau, J. Cereal Sci. 18 (1993) 145.

[39] X. Rouau, M.L. El-Hayek, D. Moreau, J. Cereal Sci. 19 (1994) 259.

[40] M.J. Taylor, in: B.W.W. Grout, G.J. Morris (Eds.), The Effects of Low Temperature on Biological Systems, Edward Arnold, London, 1987, p. 3.

[41] P.L. Steponkus, in: Y.H. Roos, R.B. Leslie, P.J. Lillford (Eds.), Water Management in the Design and Distribution of Quality Foods, Isopow 7, Technomic Publishing Co., Inc., Pensylvania, 1999, p. 53.

[42] D.S. Reid, in: Y.H. Roos, R.B. Leslie, P.J. Lillford (Eds.), Water Management in the Design and Distribution of Quality Foods, Isopow 7, Technomic Publishing Co., Inc., Pensylvania, 1999, p. 87.

[43] C.M. Courtin, J.A. Delcour, J. Agric. Food Chem. 46 (1998) 4066.

[44] D. Fessas, A. Schiraldi, J. Thermal Anal. and Cal 61 (2000) 411.

[45] G. Barone, P. Del Vecchio, D. Fessas, C. Giancola, G. Graziano, J. Thermal Anal. 38 (1992) 2779.

[46] F. Franks, Biophysics and Biochemistry at Low Temperatures, Cambridge University Press, Cambridge, 1985.

[47] M. Le Meste, D. Champion, G. Roudaut, E. Contreras-Lopez, G. Blond, D. Simatos, in: Y.H. Roos, R.B. Leslie, P.J. Lillford (Eds.), Water Management in the Design and Distribution of Quality Foods, Isopow 7, Technomic Publishing Co., Inc., Pensylvania, 1999, p. 267.

[48] G. Roudaut, M. Maglione, M. Le Meste, Cereal Chem. 76 (1999) 78.

[49] G. Roudaut, M. Maglione, D. van Dusschoten, M. Le Meste, Cereal Chem. 76 (1999) 70.

[50] Y.H. Roos, Phase Transitions in Foods, Academic Press, New York, 1995.

[51] H. Bizot, P. Le Bail, B. Leroux, J. Davy, P. Roger, A. Buleon, Carbohydrate Polym. 32 (1997) 33–50.